

## Background and Goals

The increasing interest in understanding the evolution of glaciers and of their internal structure creates the necessity of developing new processing algorithms for producing structural images from space-borne synthetic aperture radar (SAR) datasets<sup>1</sup>.

In fact, the possibility of using satellite SAR data to image 3D structures over icy Earth's zones would allow the study of vast areas, which is not currently possible by air-borne acquisitions<sup>2</sup>.

The goal of this work is to create 3D SAR-image volume from data recorded over Greenland during the Advanced Land Observing Satellite (ALOS) mission using a backprojection scheme.



Figure 1: This view of Greenland's Heimdal Glacier was captured by a NASA aircraft during Operation IceBridge on October 13, 2015. Scientists have been looking underneath the ice to predict how it might move and melt in the future.

## SAR focusing and backprojection

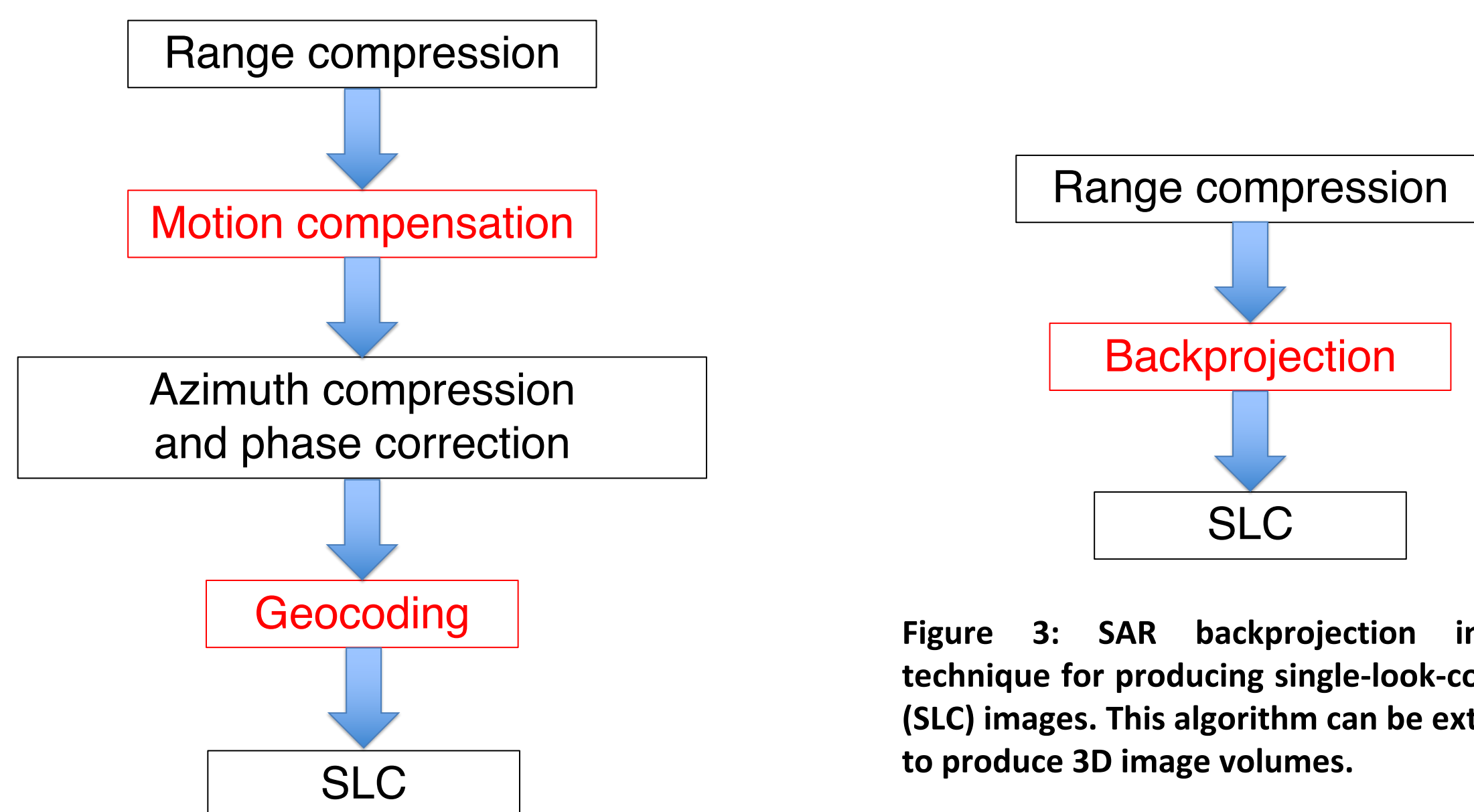


Figure 2: SAR focusing imaging technique for producing single-look-complex (SLC) images of the Earth's surface.

Figure 3: SAR backprojection imaging technique for producing single-look-complex (SLC) images. This algorithm can be extended to produce 3D image volumes.

The computational advantage of the focusing algorithm is hampered by its limitation to image surface points, unless simple planar interfaces are considered<sup>3</sup>. In addition, it relies on the following assumptions<sup>4</sup>:

- Quadratic azimuth-phase response
- Small variations of the incidence angle across range swaths
- Non-turbulent platform motion

## 3D backprojection scheme

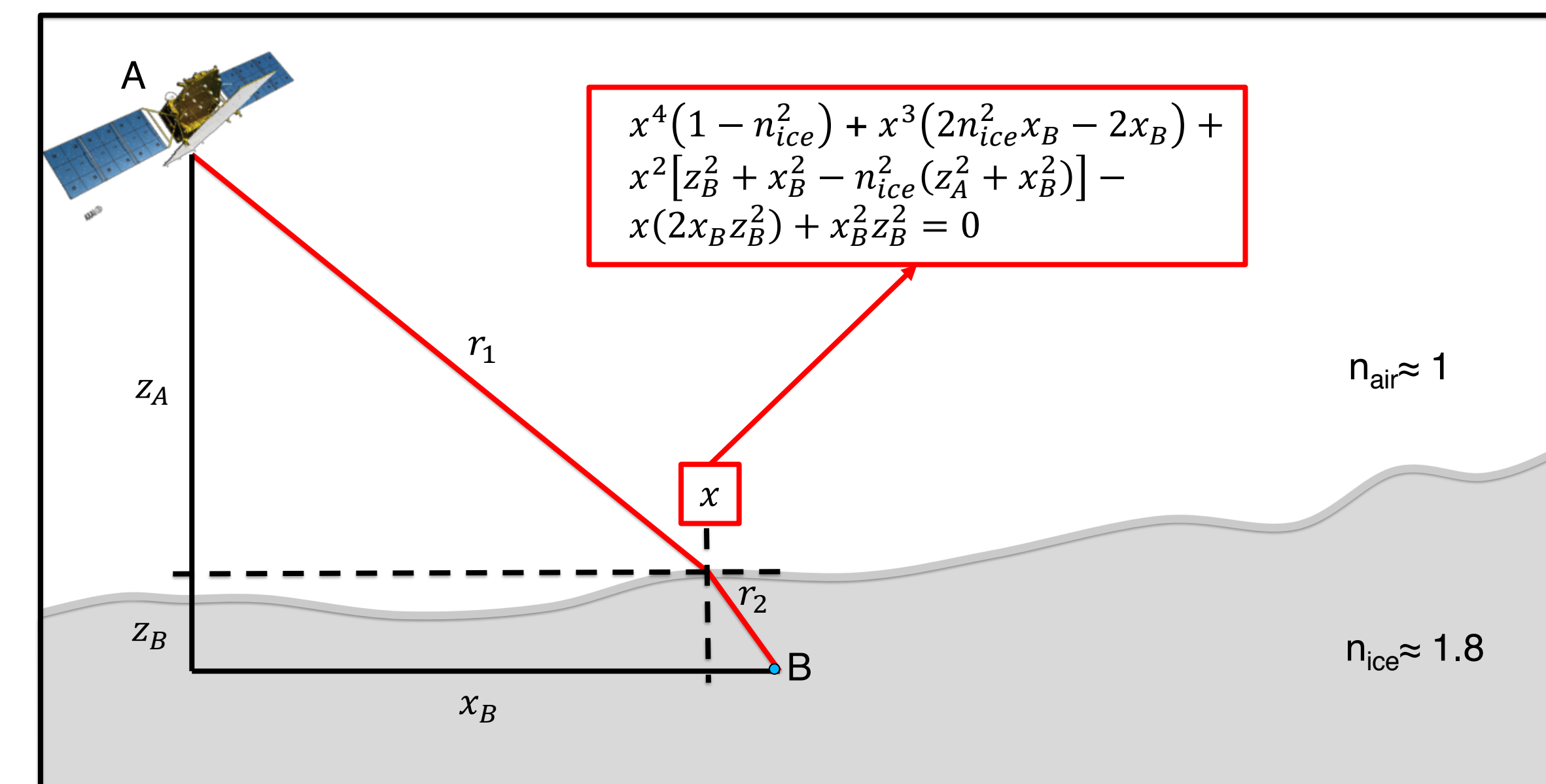


Figure 4: In the backprojection algorithm we fix the antenna and image points. Then, we sum all the energy scattered by the given image point. When imaging points below a given surface, it is necessary to consider the refraction of the incident ray.

For each image point  $\vec{p}$  and satellite position  $\vec{q}(s)$ , we need to integrate all the power  $F$  that was scattered by the considered point as follows:

$$I(\vec{p}) = \int_{s_{min}}^{s_{max}} F(s, t(\vec{p}, \vec{q}(s))) e^{\phi_p(s)} ds.$$

As long as we account for ray refraction and enough power is scattered back to the satellite, the backprojection method can be extended to produce 3D image volumes as opposed to surface-only images<sup>2-3</sup>.

## Results

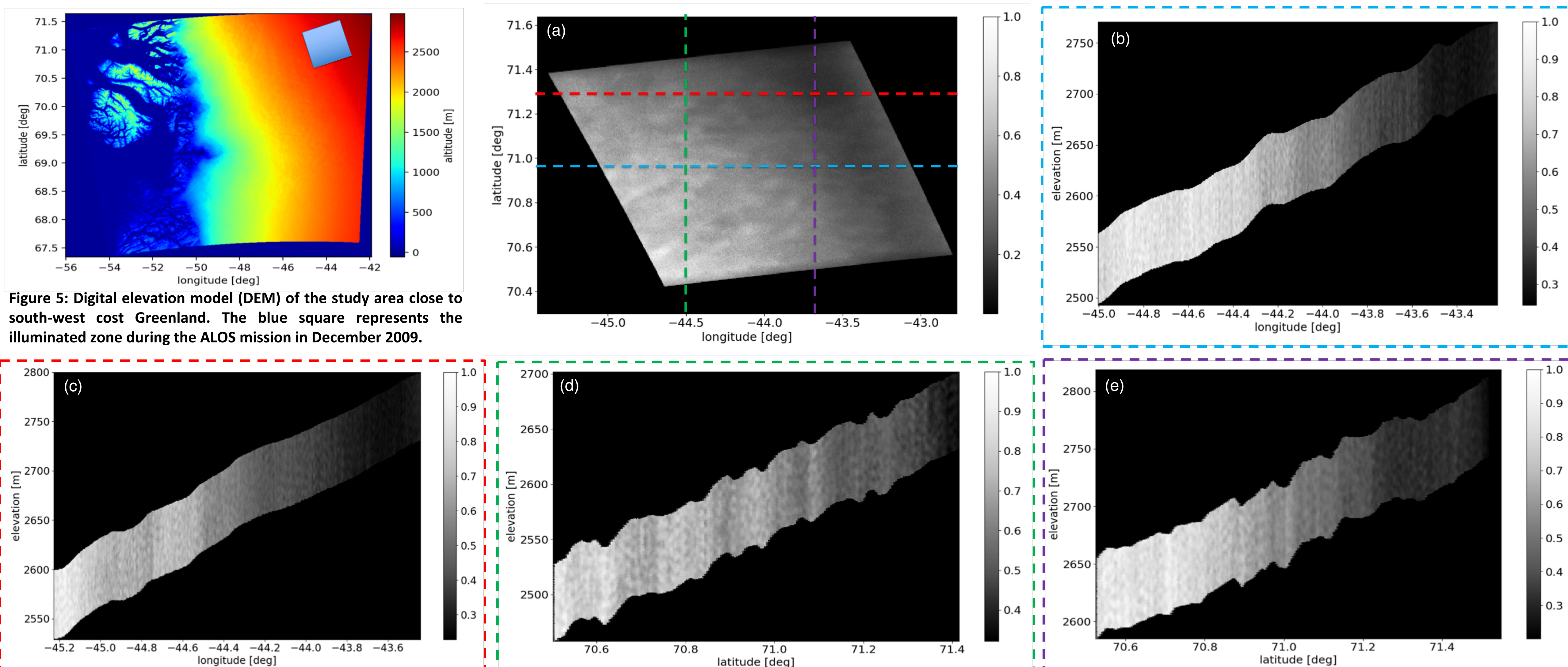


Figure 5: Digital elevation model (DEM) of the study area close to south-west coast Greenland. The blue square represents the illuminated zone during the ALOS mission in December 2009.

Figure 6: 3D backprojection results of the area shown in Figure 5. (a) Constant depth section at 20m below the air-ice interface. (b-c) Constant latitude sections at 70.96° and 71.3° lat, respectively. (d-e) Constant longitude sections at -44.56° and -43.66° lon, respectively. The pixel size is 30m by 30m in the latitude and longitude, instead the sampling in the depth direction is 0.5m. A maximum depth of 70m below the air-ice interface is considered in the shown sections

## GPU implementation

It is possible to diminish the backprojection computational cost by taking advantage of the embarrassingly parallelizable nature of the algorithm<sup>5</sup>. In fact, each image point is independent from one another.

In the shown example, we employed a NVIDIA V100 graphic processing unit (GPU) to process the data. Compared to the same algorithm run on a single multicore CPU (Intel Xeon CPU E5-2698), we are able to achieve a speedup factor of 20x.

## Conclusions and future work

- We implemented a backprojection algorithm that is able to create 3D SAR image volumes from space-borne datasets
- We applied the processor to produce a 3D image of an icy area in Greenland using ALOS mission SAR data
- We take advantage of the parallelizable nature of the algorithm and employ GPUs to decrease the processing time
- We will test the algorithm on Sentinel<sup>1</sup> data and implement an illumination compensation to correct for geometrical spreading

## References

- [1] A. Rucci, et al., 2012, Rem. Sensing of Env., Vol. 120 [2] F. Heliere, et al., 2007, IEEE TGRS, Vol. 45 [3] F. Banda, et al., 2015, IEEE TGRS, Vol. 54 [4] H. A. Zebker, et al., 2010, IEEE TGRS, Vol. 48 [5] A. Fasih and T. Hartley, 2010, IEEE Rad. Conference